104 (2025) 104921

Contents lists available at ScienceDirect

Poultry Science

journal homepage: www.elsevier.com/locate/psj

Chicken intestinal organoids reveal polarity-dependent replication dynamics and immune responses of low pathogenic avian influenza viruses

Dai-Lun Shin [a,1], Yi-Bei Tsai [a,b,1], Shu-Han Hsu [b], Chi-Chia Liang [b], Nai-Huei Wu [b,*]

[a] Department of Veterinary Medicine, National Chung Hsing University, Taichung City 402, Taiwan
[b] Department and Graduate Institute of Veterinary Medicine, National Taiwan University, Taipei City 106, Taiwan

ARTICLE INFO

Keywords:
Avian influenza virus
Intestinal organoid
Innate immune response

ABSTRACT

Low pathogenic avian influenza viruses (**LPAIVs**) persist in poultry populations, posing an ongoing challenge to poultry management and research. These viruses typically cause mild infections but can lead to significant economic losses due to their widespread presence and potential to disrupt poultry production. Traditional *in vivo* and *in vitro* models struggle to accurately replicate the avian intestinal environment, where these viruses often establish infection. In Taiwan, the domestic H6N1 LPAIVs cause an endemic in the local area but still lack investigation. This study addresses this gap by utilizing advanced chicken intestinal organoid (**CIO**) systems, apical-out (**Ap-o**), and basal-out (**Ba-o**) conformations to study the unique replication kinetics and innate immune responses of LPAIVs in a physiologically relevant setting. By comparing the Taiwan specialized H6N1 strain toward the Eurasian H9N2 virus, our results demonstrate that Ap-o organoids, which mimic natural exposure to the intestinal lumen, elicit robust interferon-stimulated gene responses, particularly higher expression of downstream gene, which effectively controls viral replication against H6N1 virus. In contrast, Ba-o organoids, representing a systemic infection route, exhibited lower upstream interferon responses, reflecting a different immune response pattern in the H9N2 strain. These results confirm that CIO is a well-suited model to study LPAIV pathogenesis. It provides key insights into the host-pathogen interactions that determine viral replication and immune evasion strategies. This model deepens our understanding of LPAIV behavior in poultry and provides a valuable tool for developing more targeted and effective control strategies for poultry health management.

Introduction

Avian influenza viruses (AIVs), members of the Orthomyxoviridae family, pose significant risks to public health and the poultry industry worldwide (Kalthoff et al., 2010). These viruses are classified based on their hemagglutinin (HA) and neuraminidase (NA) subtypes. Highly pathogenic avian influenza viruses (HPAIVs), particularly H5Nx clade 2.3.4.4, have caused devastating outbreaks with high mortality rates, affecting wild birds and poultry across continents (Lee et al., 2017; Verhagen et al., 2021). This clade's genetic diversity and adaptability underscore its persistent threat to both avian and human populations (Yamaji et al., 2020).

While HPAIVs receive significant attention, low pathogenic avian influenza viruses (LPAIVs) also pose a challenge. LPAIVs often cause subclinical infections, leading to reduced egg production and serving as reservoirs for genetic reassortment, potentially giving rise to highly pathogenic strains (Yang et al., 2017). In East Asia, H6N1 in Taiwan and H9N2 across various lineages (G1, Y280, Y439, etc.) have been circulating for decades, contributing to regional endemicity and complicating control efforts (Mostafa et al., 2018). H6N1 has been endemic in Taiwan since 1972, highlighting its long-term persistence and host adaptability (Lee et al., 2006). Though classified as an LPAIV, H6N1 has zoonotic potential, with documented human infections and detections in dogs (Wei et al., 2013), emphasizing the need for continued surveillance and investigation.

LPAIVs primarily replicate in the gastrointestinal (GI) tract of avian hosts, enabling fecal-oral transmission and environmental persistence (Abd El-Hack et al., 2022). This tropism is driven by α2,3-linked sialic acid receptors on avian intestinal epithelial cells, along with localized serine proteases (TMPRSS2, Matriptase) that cleave HA for viral entry

* Corresponding author.
E-mail address: naihueiwu@ntu.edu.tw (N.-H. Wu).
[1] Equal contributions

https://doi.org/10.1016/j.psj.2025.104921
Received 11 December 2024; Accepted 16 February 2025
Available online 17 February 2025

and replication (Baron et al., 2013; Ito et al., 1997). Unlike HPAIVs, which spread systemically, LPAIVs remain localized in the GI tract, minimizing clinical symptoms and allowing infected birds to act as carriers, exacerbating flock-level transmission (Spackman, 2023). Understanding these mechanisms is crucial for developing effective control strategies.

Traditional *in vivo* models (chickens, ferrets, and mice) have been instrumental in AIV pathogenesis studies (Wilk and Schughart, 2012). However, these models fail to capture the mild nature of LPAIV infections in poultry (Umar et al., 2017). For instance, mice are highly susceptible to AIV due to α2,3-linked sialic acids in their respiratory tract, making direct comparisons to avian infections difficult (Ge and Wang, 2011). These limitations emphasize the need for advanced *in vitro* models that closely mimic the avian intestinal environment.

Recent advances in 3D culture systems have enabled the development of chicken intestinal organoids (CIOs), which provide a physiologically relevant model for studying AIV replication and host interactions (Chen et al., 2023; Nash and Vervelde, 2022). Unlike 2D cultures, CIOs retain cellular diversity and spatial organization, allowing simulation of luminal (Ap-o) and systemic (Ba-o) infection routes (Nash et al., 2021). Apical-out (Ap-o) organoids expose the apical surface, mimicking natural gut lumen interactions, while basal-out (Ba-o) organoids expose the basal surface, modeling systemic infection pathways (Wu et al., 2016). These configurations allow researchers to investigate virus-host interactions in a controlled setting.

The innate immune response is critical for early AIV defense, particularly in the avian intestinal epithelium (Abd El-Hack et al., 2022). Viral RNA is recognized by pattern recognition receptors (PRRs) such as Toll-like receptors (TLRs) and RIG-I-like receptors (RLRs), triggering type I interferons (IFN-α, IFN-β) and ISG responses (Takeuchi and Akira, 2010). However, avian species exhibit variability in ISG responses, affecting their susceptibility to AIV (Bazzigher et al., 1993; Santhakumar et al., 2017). Notably, Mx GTPases, key antiviral proteins in mammals, are less effective in birds, contributing to higher susceptibility in chickens (Ko et al., 2002). Understanding how LPAIVs persist in the avian GI tract requires studying the balance between host immunity and viral immune evasion strategies.

Materials and methods

Viruses

Original stocks of influenza viruses A/Wild duck/Ilan/2904/1999 (subtype H6N1, 2904) were obtained from Prof. Ching-Ho Wang, National Taiwan University, Taiwan. The A/chicken/Emirates/R66/2002 (H9N2, R66) was provided by Prof. Georg Herrler, University of Veterinary Medicine Hannover, Germany, and the generation of the virus was described in our previous study (Yang, et al., 2017). The viruses were propagated in the chorio-allantoic cavity of 9-day-old SPF embryonated chicken eggs for three days (Brauer and Chen, 2015). The allantoic fluid was harvested, aliquoted, and stored at −80°C. The viral titer was determined using a focus-forming assay. The H6N1-2904 virus was used to represent the common viral pathogens in the East Asia region, especially in the poultry industries of Taiwan. Conversely, the H9N2-R66 virus represents the common Eurasian H9N2 G1 virus circulating for decades.

Immortalized and primary intestinal cell culture

Immortalized Caco-2 and MDCK cells were maintained in a DMEM medium containing 10 % FBS. Cells were cultivated and passed twice per week until the experiment. As for the primary intestinal epithelial stem cells, the procedure is as follows: Euthanize 18-day-old specified pathogen-free (SPF) chicken embryos (JD-SPF Biotech Co., Ltd., Miaoli, Taiwan) using CO_2. After euthanasia, remove the small intestine and cut it into small pieces using a surgical scissor. Rinse the small intestine sections multiple times with phosphate-buffered saline (PBS) until the washing buffer remains clear and collect the fragments in a 50 ml centrifuge tube, supplied with 10 ml of 5 mM EDTA (Thermo Fisher Scientific Inc., USA), incubate at 37°C for 5 min. Followed by mixing the materials in a rotatory shaker for 30 to 40 min at room temperature. Centrifuge the mixture at 450 xg at 4°C for 5 min and discard the unwanted supernatant. Rinse the small intestine fragments with 10 ml of PBS containing 0.1 % bovine serum albumin (BSA; Bioman Scientific, Taiwan) to isolate the intestinal epithelial cells. Filter the collected supernatant through a 70 μm cell strainer (Falcon, USA) to remove large cell debris. Repeat this step 5 times. The primary intestinal epithelial stem cells can be obtained from the cell suspension collected from the 3rd to 5th washing/collection step (Lee, et al., 2018; Pierzchalska, et al., 2012).

Organoid expansion

The collected intestinal stem cells were centrifuged prior to expansion and resuspended the cells within the expansion mixture between the organoid expansion medium (EM) and extracellular matrix (ECM) Matrigel® (Corning, USA) at a 1:1 ratio. The organoid expansion medium (EM), which consists of Advanced DMEM/F-12 (Thermo Fisher Scientific Inc., USA) supplemented with the following components: 50 μg Primocin (InvivoGen, USA), Penicillin-Streptomycin (Thermo Fisher Scientific Inc., USA), B27 (Thermo Fisher Scientific Inc., USA), 10 mM Nicotinamide (Sigma-Aldrich, Germany), 500 nM A83-01 (Sigma-Aldrich, Germany), 10 μM SB202190 (Sigma-Aldrich, Germany), 50 ng/ml EGF (Corning, USA), 10 μM Y27632 (Sigma-Aldrich, Germany), 1 mM N-acetyl-l-cysteine (NAC, Sigma-Aldrich, Germany), L-WRN Conditioned Media Supplement (Sigma-Aldrich, Germany). Additionally, either 20 μM PGE2 or 10 nM Gastrin (Sigma-Aldrich, Germany) is added for comparison. Transfer the cells into a pre-warmed 24-well plate at 5×10^3 cell clumps/50 μL/well. Place the 24-well plate in a 39 °C, 5 % CO_2 incubator for about 30 min, allowing the Matrigel to solidify. Slowly add 500 μL of EM to each well and incubate in a 39°C, 5 % CO_2 incubator. Change the EM every 3 days. The clumps will form organoids within 4 to 5 days of culture in the EM. Similar procedures were used to form the Caco-2 organoids, only 10 nM Gastrin but PGE2 were not used in the Caco2-EM.

Differentiation of intestinal organoids

When the expansion organoids reach a size of more than 200 μm, they can be induced to differentiate. Both Caco2-derived and primary chicken intestinal epithelial cell-derived organoids (CIO) were performed by following procedures. Remove the EM and gently rinse the wells once with PBS. Add 500 μL of PBS to each well, and gently disrupt the Matrigel with a pipette tip. Collect all organoids into a 15 mL centrifuge tube and centrifuge at 450 xg at 4°C for 5 min, then discard the supernatant. Add 1 mL of TrypLE™ Express Enzyme (Thermo Fisher Scientific Inc., USA), incubate at 37°C for 5 min, and then stop the enzymatic reaction with 4 mL of ice-cold DMEM. Disperse the cells again and centrifuge at 450 xg at 4 °C for 5 min. Discard the supernatant to obtain the dissociated cell fragments. Based on the desired cell morphology, two methodologies were applied:

Basal-out (Embedded in ECM): Resuspend the dissociated cell fragments in EM and Matrigel at a 3:7 ratio and follow the same steps as for organoid expansion. The next day, replace the medium with differentiation medium (DM), and after about 6 to 8 days of culture, the organoids will be fully differentiated. The differentiation medium (DM) consists of Advanced DMEM/F-12 supplemented with 50 μg Primocin, Penicillin-Streptomycin, B27, 10 nM Gastrin, 500 nM A83-01, 50 ng/ml EGF, 10 μM Y27632, 1 mM NAC.

Apical-out (Suspension Culture): Resuspend the dissociated cell fragments in 5 mL of 1 mM EDTA and place them on a rotating platform at 4°C for 1 h to completely remove the residential Matrigel. Centrifuge

the mixture at 450 xg at 4°C for 5 min, discard the supernatant, and wash the cells with 5 mL of DMEM. Centrifuge again at 450 xg at 4°C for 5 min, discard the supernatant, and resuspend the cells in DM. Transfer 400 μL of the suspension into a 24-well plate and incubate at 39 °C with 5 % CO_2. Change the medium every 3 days, and after about 8 to 10 days of culture, the organoids will be fully differentiated (Beaumont, et al., 2021; Nash, et al., 2021).

Low pathogenic avian influenza virus infection

In order to infect the organoids with H9N2 and H6N1 influenza viruses, both basal-out and apical-out organoids were washed 2 times with PBS and inoculated with 1×10^5 FFU/500μL viruses at the density of 100 organoids per well. After inoculating for 2 h at 39°C, the organoids were washed 3 times with PBS to eliminate any residual viruses. The supernatant was collected at 2, 24, 48, and 72 hpi for virus titration through the focus-forming assay. Organoids were harvested at 24 hpi for quantitative reverse transcription polymerase chain reaction (qRT-PCR) to evaluate mRNA transcript expression levels. Furthermore, organoids were fixed in 4 % paraformaldehyde (PFA) at 24 and 72 hpi for immunofluorescence microscopy staining (Wu, et al., 2016)

Immunofluorescence staining

Organoids were fixed for 30 min in 4 % PFA, permeabilized for 40 min in 0.5 % Triton X-100 (Sigma-Aldrich, Germany), and blocked for 1 h in 5 % goat serum at 37 °C. Organoids were then incubated with primary antibodies diluted in the blocking buffer overnight at 4°C, followed by incubation with secondary antibodies for 2 h at room temperature. Nuclei were stained by DAPI (4′,6-diamidino-2-phenylindole) for 20 min and were embedded with ProLong™ Gold Antifade Mountant (Thermo Fisher Scientific Inc., USA). All samples were imaged on a fluorescence microscope (Zeiss Axio Observer 7, Germany) and processed using ZEN software version 3.5. In this study, the following primary antibodies were used: a mouse anti-influenza A nucleoprotein (NP) monoclonal antibody (Bio-Rad, USA), mouse anti-mucin-5AC monoclonal antibody (Thermo Fisher Scientific Inc, USA), mouse anti-ZO-1 monoclonal antibody (Thermo Fisher Scientific Inc, USA), Cy3-labeled phalloidin (Thermo Fisher Scientific Inc, USA), rabbit monoclonal recombinant anti-villi antibody and rabbit anti-β-catenin antibody (Sigma-Aldrich, Germany). Secondary antibodies goat polyclonal antibodies against mouse or rabbit IgG were conjugated with Alexa Fluor® 488 or 568 (Thermo Fisher Scientific Inc, USA) (Wu, et al., 2016).

Lectin staining

Organoids were fixed for 30 min in 4 % PFA and blocked for 1h in Streptavidin/Biotin Blocking Solution (Thermo Fisher Scientific Inc., USA) at room temperature. Organoids were then incubated with biotinylated *Maackia amurensis* Lectin II (MAL-II) and *Sambucus Nigra* Lectin (SNA) conjugate with fluorescein (Vector laboratories, USA) at 4°C overnight. The organoids were incubated with Cy3-conjugated streptavidin (Sigma-Aldrich, Germany) for 2 h at room temperature. Nuclei were stained by DAPI for 20 min and were embedded with ProLong™ Gold Antifade Mountant and examined under a fluorescent microscope (Zeiss Axio Observer 7).

Virus titer determination by focus-forming assay

To quantify viral replication in the organoids, the inoculated DMEM, along with organoid samples, were collected and processed. Viral titers expressed as focus-forming units (FFU) per mL were determined on MDCK cells described previously. Briefly, MDCK cells were plated in 96-well plates, and serial 10-fold dilutions of the inoculum in DMEM containing 5 μg/mL TPCK-treated trypsin (Sigma-Aldrich, Germany) were prepared. After 24 h of incubation at 37 °C, cells were washed and fixed with 4 % formaldehyde. Cells were then permeabilized using a buffer solution of 0.5 % Triton X-100 and 20 mM glycine in PBS. Following permeabilization, the cells were incubated with a mouse monoclonal antibody against influenza nucleoprotein (Bio-Rad) and subsequently treated with an HRP-conjugated goat anti-mouse IgG secondary antibody (SeraCare KPL). The immunological staining was performed using the TrueBlue substrate (SeraCare KPL), and the resulting foci were counted to calculate FFU per well. The assay detection threshold was set at 200 infectious units, and for samples without detectable foci, data points were adjusted to 50 FFU (Shin, et al., 2020).

qRT-PCR for detecting chicken innate immune biomarkers

Quantitative real-time PCR was used to assess mRNA expression levels in H9N2 or H6N1 AIV-infected CIOs. The CIOs were infected with the virus, as in the infection study above. After 24 h post-infection (p.i.), the total RNA was extracted using the RNeasy Minikit® following the manufacturer's protocol (Qiagen). The one-step real-time PCR was carried out on a LightCycler 96 system (Roche, Switzerland) using the QuantiTect SYBR® Green RT-PCR Kit (Qiagen) per the manufacturer's guidelines. The primers used for detecting chicken *Mx1, IFNα*, and *β-actin* transcripts are listed in Table 1, with β-actin serving as the housekeeping gene control. The M gene of the influenza virus had been included to quantify the amount of viral particles harbored by organoids. To quantify the viral load of LPAIV in CIOs, M-gene RNA copies per sample were measured using qRT-PCR, following the method described in (Delgado-Ortega, et al., 2014). The relative expression of target genes was determined using the $2-\Delta\Delta CT$ method and presented as fold changes relative to mock-infected controls (Shin, et al., 2020).

In our study, the release of infectious viral particles of H9N2-R66 and H6N1-2904 was quantified using the focus-forming assay (FFU), while qRT-PCR measured Flu M-gene copies, which represent total viral RNA—including both released and intracellular viral genomes. These two methods are mainly positively correlated but reflect different aspects of viral replication.

Statistical analysis

All data were analyzed using GraphPad Prism 9 (GraphPad Software, California). Results are expressed as mean values ± standard error of the mean (SEM). Statistical comparisons between the two groups were made using the Mann-Whitney U test. For multiple group comparisons, statistical significance was determined using Tukey's post-hoc test. Pearson's R correlation analysis was implied to compare the data set between the different formats of organoids. Genetic analysis was carried out through the GISAID EpiFlu™ platform for accessing sequence data. The immunofluorescent images were taken by Zeiss Axio Observer 7.

Table 1
Primers used for quantitative real-time PCR.

Target gene	Primer name	Sequence	Reference
chicken *Mx1*	ch*MX1*-F	CACACCCAACTGTCAGCGAT	(Deblanc, et al., 2016)
	ch*MX1*-R	ATGTCCGAAACTCTCTGCGG	
chicken IFNα	chIFNa-F	CCAGCACCTCGAGCAAT	(Li, et al., 2013)
	chIFNa-R	GGCGCTGTAATCGTTGTCT	
chicken β-Actin	chBAct-F	AGCGAACGCCCCCAAAGTTCT	(Hassanpour, et al., 2018)
	chBAct-R	AGCTGGGCTGTTGCCTTCACA	
Influenza M gene	M52C	CTTCTAACCGAGGTCGAAACG	(Fouchier, et al., 2000)
	M254R	AGGGCATTTTGGACAAAKCGTCTA	

Ethic

The ethical consideration of animal experiment procedure has been approved by the Institutional Animal Care & Use Committee (IACUC) of National Taiwan University, Taiwan (IACUC Approval No: NTU-110-EL-00124).

Results

Establishment and expansion of chicken intestinal organoids

We successfully established chicken intestinal organoids (CIOs) in two distinct formats: Ba-o and Ap-o CIO. The CIOs were derived from intestinal stem cells isolated of 18-day-old SPF embryos. These stem cells were embedded in Matrigel and cultured with an L-WRN-supplemented medium, leading to the formation of organoids within 4-6 days. To optimize growth, we compared the effects of PGE2 and Gastrin as supplemental growth factors, for further application.

Our results demonstrated that PGE2 significantly enhanced the expansion of CIOs, promoting the formation of organoids that could grow up to approximately 300 μm in diameter and maintain viability over multiple passages. Conversely, organoids cultured with Gastrin exhibited poor growth, with increased apoptosis and fragmentation observed as early as the third day of culture. These findings suggest that PGE_2 is superior to Gastrin for the expansion and maintenance of chicken intestinal organoids (Fig. 1).

Although previous studies had shown that PGE2 was suitable for chicken intestinal organoids formation, however, comparing side by side toward common usage of Gastrin supplement, such as Caco2-organoids formation, had yet been validated. We suggest that only in the expansion period should the PGE2 be included, and the protocol using L-WRN for simple Wnt-3A, R-spondin 3, and noggin source would be a more suitable method for growing chicken intestinal organoids. Additionally, despite challenges in removing fibroblasts using CHIR99021, the cultures stabilized after three passages, allowing us to focus on the differentiation and functional characterization of the organoids.

Differentiation expansion CIO into Ba-o and Ap-o CIOs

We further differentiated the CIOs into two formats: Ba-o and Ap-o CIO. The Ba-o CIOs, cultured within Matrigel, developed inward-growing villi resembling the natural intestinal lumen. In contrast, the Ap-o CIO, cultured in suspension, exhibited outward villi growth, exposing the apical surface to the medium, which is critical for interactions with luminal pathogens (Fig. 2A-B).

Immunofluorescence staining confirmed the presence of key cell marker, villi (Fig. 3A-B), and specific cell-cell junction proteins, including β-catenin (Fig. 3A-B), ZO-1, and F-actin (Fig. 3C-D), in both formats. The Ap-o CIO, in particular, displayed intact junctions and well-differentiated villus structures, indicating that they accurately recapitulate the architecture and barrier functions of the intestinal epithelium. This makes them particularly suitable for studying pathogen interactions.

Influenza virus infection of chicken CIOs

To assess the suitability of CIOs for avian influenza virus infection studies, we infected both Ba-o and Ap-o CIOs with H6N1-2904 and H9N2-R66 strains and used Caco-2 organoids (also apical-out and basal-out format) as control. After collecting the organoids together with the culture medium, the virus titer was determined using a focus-forming

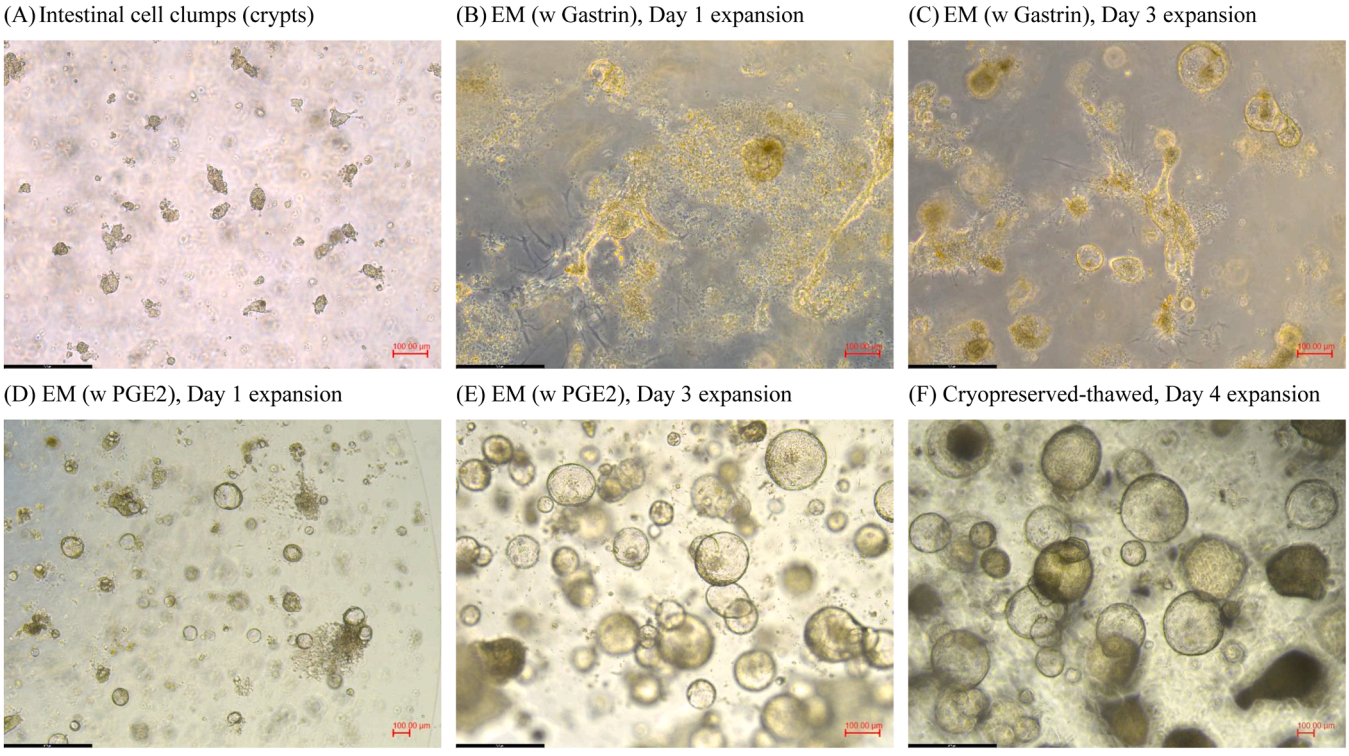

Fig. 1. Establishment of Chicken Intestinal Organoids (CIOs) Using PGE2 or Gastrin. The Figure illustrates the establishment and growth of chicken intestinal organoids (CIOs). The initition materials, cell clumps (crypts) isolated from chick intestinal epithelium surface (A). Primary chicken intestinal cells culture with the expansion medium (EM) using gastrin (day 1: B, day 3: C); or expansion medium supplied with PGE2 (D-F). The results demonstrate that PGE2 significantly enhances organoid expansion (day 1: D, day 3: E), resulting in larger, more stable spheroids compared to Gastrin, which led to poor growth and increased apoptosis. Organoids cultured with PGE2 suppled EM formed enteroids up to 300 μm in diameter and maintained viability over multiple passages, and the cryopreserved materials can be expanded after proper thaw and culture procedure (F). Scale bar: 100 μm.

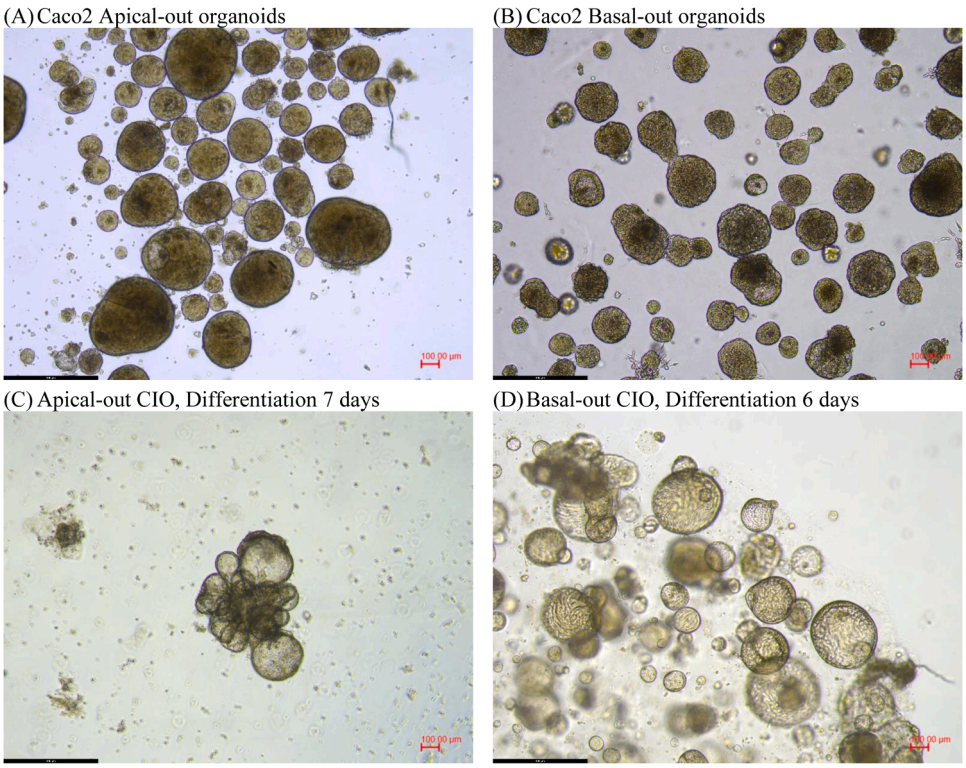

Fig. 2. Differentiation of Ap-o and Ba-o CIOs. These cultures were examined under the inverted phase-contrast light microscope (DMi1, Leica Germany). The Fig. shows the differentiation of Caco2-derived organoids and CIOs into Ba-o (basal-out) and Ap-o (apical-out) formats. Caco2-derived organoids were used to represent a standard formation of steroid cultures (A-B). The Ap-o CIOs cultured in suspension DM exhibited outward villi growth on day 6 differentiation, containing the apical surface exposed to the medium (C). The Ba-o CIOs cultured in matrigel developed inward-growing villi (D). Scale bar: 100μm.

assay. Our findings revealed that both formats supported viral replication despite differing efficiencies.

The Ap-o and Ba-o CIOs were particularly effective at mimicking *in vivo* conditions, allowing virus entry and replication without the need for exogenous TPCK-treated trypsin, Different from the CaCo-2 cells organoids, which were susceptible to H6N1-2904 virus in the Apical-out format but not access the virus to infect via basolateral surface (Fig. 4A-D). In the Ap-o and Ba-o CIOs, viral titers of H6N1-2904 and H9N2-R66 viruses remained stable at approximately 10^4 FFU/ml, while in apical-out CaCo2 cells, titers reached up to 10^6 FFU/ml (Fig. 4A).

Interestingly, the Ba-o CIOs supported higher viral titers (up to 10^5 FFU/ml) by 48 h post-infection (h.p.i.) in both H6N1-2904 and H9N2-R66 viruses compared to Ap-o CIOs, suggesting that the basolateral side of the intestinal epithelium may provide a more conducive environment for AIV replication (Fig. 4B).

Sialic acid expression and its role in viral entry

Lectin staining revealed that on the surface of Ap-o CIO, the α2,3-linked sialic acids, as known as the avian influenza virus receptor, are abundantly expressed. Partial regions show co-expression of α2,6-linked sialic acid, which is mainly the receptor for human influenza viruses (Fig. 5). This dual expression is significant as it allows these organoids to model interactions with both avian and human-tropic influenza viruses. However, while lectin staining provides evidence of sialic acid receptor distribution, it does not directly visualize viral entry. Since lectins require an intact plasma membrane for staining, viral particles that have already entered the cytoplasm are not detectable using this method.

Differential immune response to AIV infection

Our analysis of the immune response to AIV infection in CIOs revealed differential activation of interferon-stimulated genes (ISGs) depending on the viral strain and organoid format. In Ap-o CIO infected with the H9N2-R66 strain, there was no significant activation of ISGs, suggesting inhibition of the downstream IFN pathway, possibly through blockade of the STAT signaling route. This indicates a potential mechanism by which H9N2-R66 may evade host immune responses (Fig. 6A).

In contrast, the H6N1-2904 strain induced a robust ISG response in Ap-o CIO, yet the viral M gene copy number remained high, indicating ongoing viral replication despite the immune activation. These findings suggest that H6N1 may balance its replication with host-defense mechanisms, allowing it to persist within the intestinal epithelium without overwhelming the host's immune system (Fig. 6B). Interestingly, comparing the expression profile in the infected Ba-o CIOs, the H9N2-R66 virus stimulates more ISGs compared to the H6N1-2904 virus, which may be reflected in the route of virus entry, that persistent infection of H6N1-2904 via the bloodstream (mainly basal infection) does not trigger the innate immune response of intestines.

Comparative analysis of Ba-o and Ap-o CIO in AIV infection

To further examine the differences in Ba-o and Ap-o CIOs, we analyzed trends in viral replication and immune responses (Fig.s 4 and 6), supported by Pearson's r-correlation analysis (Fig. 7). The results indicated that H6N1-2904 exhibited lower replication in Ap-o organoids than in Ba-o organoids, which correlated with higher ISG expression in Ap-o CIOs. In contrast, H9N2-R66 displayed higher viral titers in Ba-o organoids, where the ISG response was less pronounced, suggesting that the innate immune response, rather than organoid orientation alone, plays a key role in modulating viral replication dynamics.

The correlation analysis further reinforced this observation by revealing a strong inverse relationship between ISG expression and viral titers across different conditions. A significant negative correlation was observed between Mx1 expression and FluM levels in H9N2-R66 Ap-o CIOs ($r = -0.87$, $p = 0.0002$) and Ba-o CIOs ($r = -0.85$, $p = 0.0004$), as

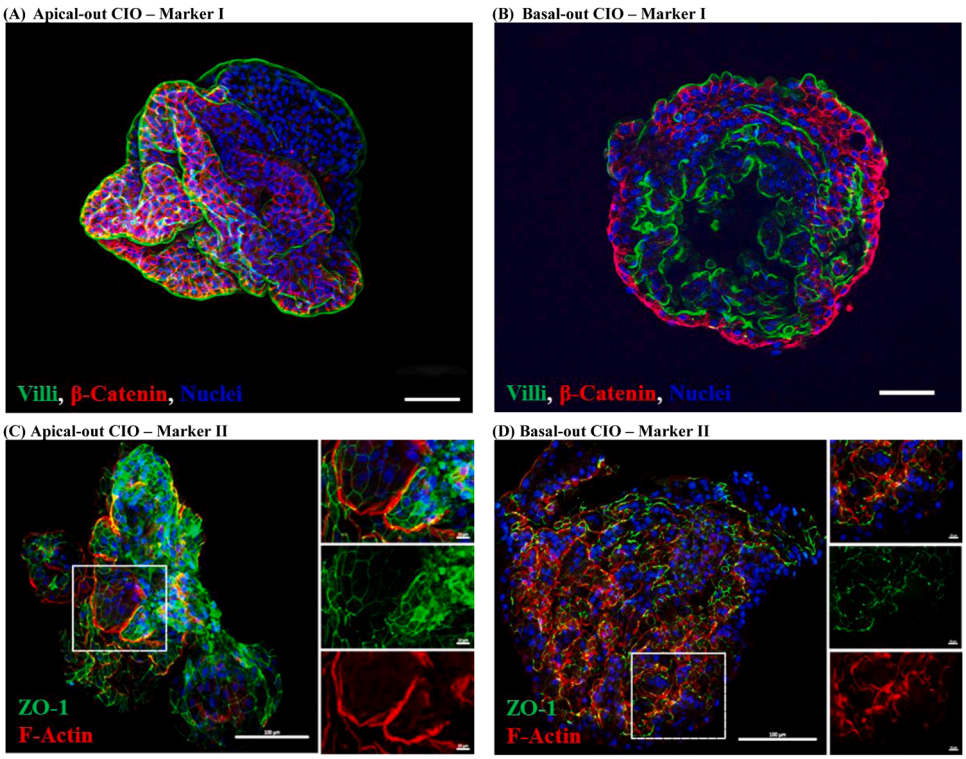

Fig. 3. Characterization of well-differentiated CIOs via Immunofluorescence. The fixed CIOs were examined by using a fluorescence microscope after immunofluorescence staining. The differentiation of CIOs into Ba-o (basal-out) and Ap-o (apical-out) formats had been visualized by examining specific cell markers. Ap-o CIOs cultured in suspension exhibited outward villi (green), growth with the apical surface exposed to the medium (A), while Ba-o CIOs cultured in Matrigel developed inward-growing villi (B). Immunofluorescence staining confirmed the presence cell marker Villi (upper panel, green), and of crucial junction proteins, including β-catenin (upper panel, red), ZO-1 (bottom panel, green), and F-actin (bottom panel, red), indicating intact cell-cell junctions and proper epithelial architecture. The zoom-in vision of the dash square area had been shown accordingly for Ap-o (C) and Ba-o CIOs (D). Scale bar: 100μm (A-B, C-D left panel); 10μm (C-D zoom-in panel).

well as in H6N1-2904 Ba-o CIOs ($r = -0.7$, $p = 0.01$). This statistical relationship underscores the role of antiviral immune activation in suppressing viral replication, irrespective of epithelial polarity. While orientation influences viral entry, these findings suggest that host immune responses are a major determinant of viral replication control in intestinal organoid models.

This study established both Ba-o and Ap-o CIOs as a versatile model for avian influenza research. The observed differences in immune responses and viral replication provide insights into AIV persistence in the intestinal epithelium, highlighting CIOs as a valuable tool for studying pathogenesis and antiviral strategies.

Discussion

Avian influenza viruses (AIVs) encompass diverse pathogens with broad variation in host range and tissue tropism. H6N1 LPAIV has been enzootic in Taiwan since 1976 and became more prevalent after the emergence of HPAIV in 1997 (Lee, et al., 2006). Studies have shown that H6N1 virus can cause up to a 33 % reduction in egg production and a 3.8 % mortality rate in affected flocks (Wang and Wang, 2003). The H6N1-2904 virus, originally isolated from the same region as A/DK/Taiwan/WB29/99, harbors the original 228G in its HA protein, which has been linked to avian adaptation (Lee, et al., 2006; Wei, et al., 2013). While direct chicken challenge studies using the H6N1-2904 strain are unavailable, previous experiments with other Taiwanese H6N1 strains (1999-2005) demonstrated that they did not induce overt clinical symptoms in chickens (Ou, 2003). However, more recent studies have shown that evolved H6N1 strains with HA mutations, such as G228S, can exhibit nephrotropism and cause interstitial nephritis in experimentally infected chickens (Tu, et al., 2022).

Similarly, the H9N2-R66 strain has been widely used in studies on viral reassortment and genetic drift in LPAIV (Gohrbandt, et al., 2011; Peacock, et al., 2021; Penski, et al., 2011; Yang, et al., 2017). Previous *in vivo* experiments involving oral-nasal inoculation of chickens with H9N2-R66 revealed that infected chickens exhibited no apparent symptoms but shed through both aerosol and fecal-oral transmission routes, as confirmed by viral detection in oral and cloacal swabs (Gohrbandt, et al., 2011; Penski, et al., 2011). These findings suggest that H9N2-R66 can replicate in gastrointestinal and respiratory tracts. Therefore, our study, which utilizes CIOs to assess LPAIV pathogenicity in gastrointestinal organs, provides a relevant platform for investigating viral-host interactions in a controlled system.

The hemagglutinin (HA) glycoprotein on the surface of LPAIV mediates host cell entry by binding to α2,3-linked sialic acids, which are abundant in the avian gastrointestinal (GI) tract. This sialic acid specificity, combined with limited α2,6-linked binding, drives the virus's tropism toward intestinal tissues in birds (Shinya, et al., 2006). Previous studies have demonstrated that H6N1 primarily targets α2,3-linked sialic acids (MAA) with limited affinity for α2,6-linked sialic acids (Wei, et al., 2013), while H9N2-R66 also preferentially binds α2,3-linked sialic acids (Yang, et al., 2017). Given that Ap-o CIOs exhibit robust α2, 3-linked sialic acid expression, they serve as a relevant model for studying AIV binding and early entry events. This GI tropism has led to the development of *in vitro* models, such as chicken intestinal organoids (CIOs), which closely replicate the avian intestinal environment (Huang, et al., 2017).

Compared to the *in vitro* models, traditional animal models, such as chicken and BALB/c mice infection studies, have been used for decades to evaluate the pathogenicity of HPAIVs and also LPAIV research which showed their limitations. LPAIVs often induce minimal symptoms in

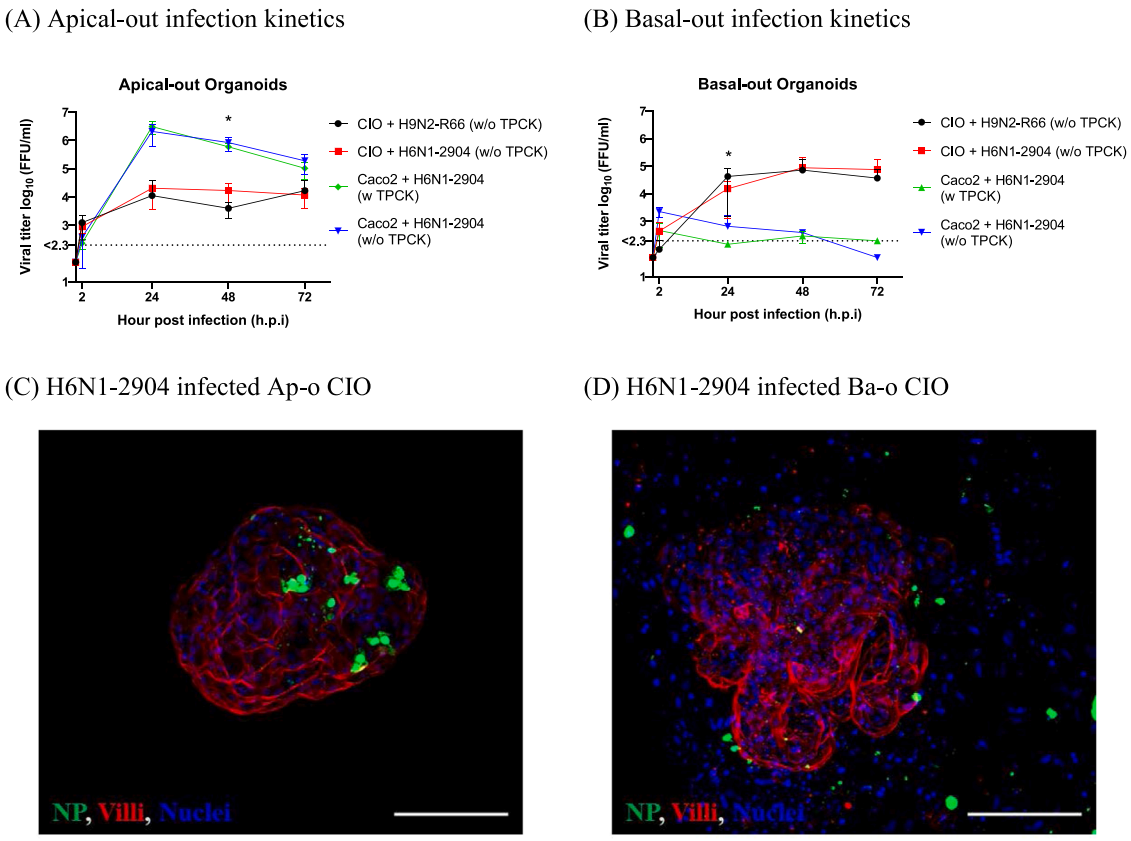

Fig. 4. Viral Replication Kinetics in Ba-o and Ap-o CIOs. The viral replication kinetics of the H9N2-R66 and H6N1-2904 strains in Ba-o, Ap-o CIOs, and Caco2 organoids. All CIOs were inoculated directly with LPAIVs (H9N2-R66 and H6N1-2904) without the addition of TPCK-treated trypsin (w/o TPCK). In contrast, Caco-2 organoids, including both Ap-o and Ba-o forms, were infected either with (w TPCK) or without (w/o TPCK) the addition of TPCK-treated trypsin during the experiments. Ba-o CIOs supported higher viral titers (up to 10^5 FFU/ml) compared to Ap-o CIOs, emphasizing the influence of the epithelial orientation on viral replication dynamics (A-B). The results were shown as means ± SD of nine CIOs (Ap-o & Ba-o). Statistical comparisons of viral titers between H9N2-R66 and H6N1-2904 in Ap-o and Ba-o organoids at different time points were performed using Tukey's multiple comparisons test (***$P < 0.001$, **$P < 0.01$, *$P < 0.05$). Immunofluorescence staining of virus nucleoprotein in CIOs on day 1 post-H6N1-2904 infection was visualized (Ap-o CIO: C, Ba-o CIO: D). The monoclonal mouse antibodies against influenza viral nucleoprotein were visualized by recognizing an Alexaflour 488 conjugated secondary antibody (NP, Green), and villi (red) were visualized to represent the location of the viral particles. Scale bar: 100μm.

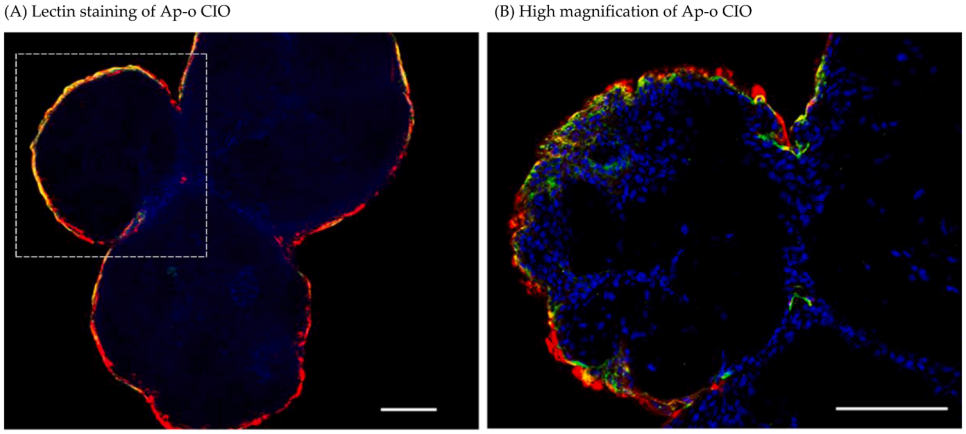

Fig. 5. Sialic Acid Expression on Ap-o CIOs. This figure shows the lectin staining of Ap-o CIOs, demonstrating the expression of both α2,3- and α2,6-linked sialic acids on the apical surface. The stained SNA showed in green, while MAAII conjugated with Cy3 stained in red indicates the α2,6-linked sialic acid and α2,3-linked sialic acid expression, respectively (A). The zoom-in picture is shown in the right panel (B). The dual expression pattern allows these organoids to serve as a model for studying the binding and entry of both avian- and human-tropic influenza viruses, while the α2,3-linked sialic acid, known as avian influenza virus receptor, showed dominant expression pattern. Scale bar: 100μm.

chickens, making it challenging to characterize host-pathogen interactions fully (Weerts, et al., 2022). Studies using BALB/c and other mouse strains demonstrate susceptibility to LPAIV, with high mortality rates linked to the binding of α2,3-linked sialic acids in the airways (Kanrai, et al., 2016; Wu, et al., 2015), which limits these models' ability to represent the natural course of LPAIV infections in birds accurately

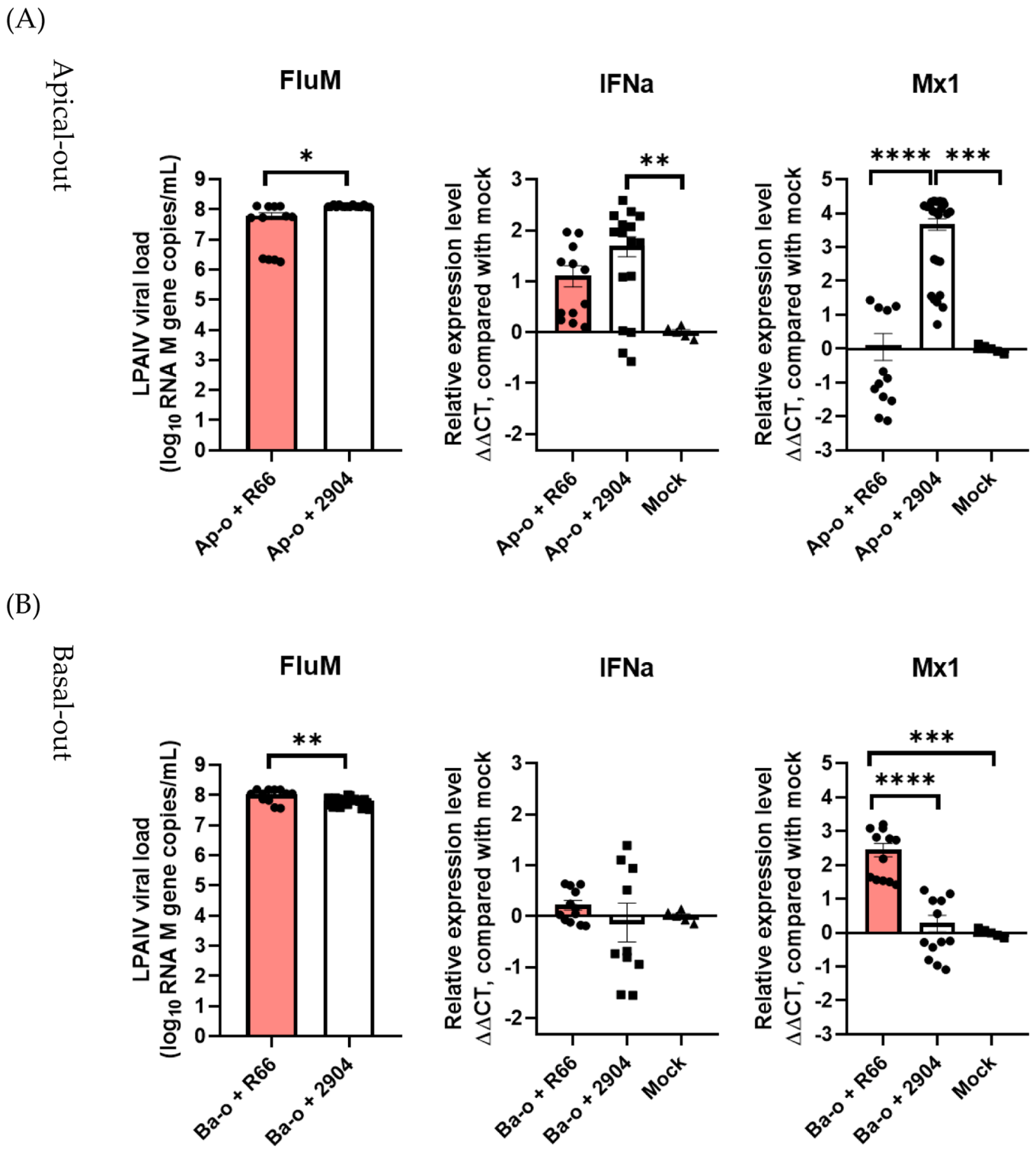

Fig. 6. Differential Immune Response to AIV Infection in CIOs. The figure illustrates the differential activation of interferon-stimulated genes (ISGs) in response to AIV infection in Ap-o and Ba-o CIOs (A & B). The FluM quantified by M gene qRT-PCR indicated relatively quantified virus particles, shown in log10 RNA M gene copies/mL. The upper stream of the interferon stimulation pathway was evaluated by monitoring the expression level change of chicken IFNα in the infected organoids. The downstream ISGs were detected by the chicken *Mx1* gene, representing the activation of downstream ISG expression. The H9N2-R66 strain did not significantly activate ISGs, suggesting inhibition of the downstream IFN pathway, while the H6N1-2904 strain induced a robust ISG response, highlighting distinct viral strategies for immune evasion and persistence. The results were shown as means ± SEM of nine CIOs. Statistical analysis was performed with Statistical analysis was performed with Tukey's multiple comparisons test (***$P < 0.001$, **$P < 0.01$, *$P < 0.05$).

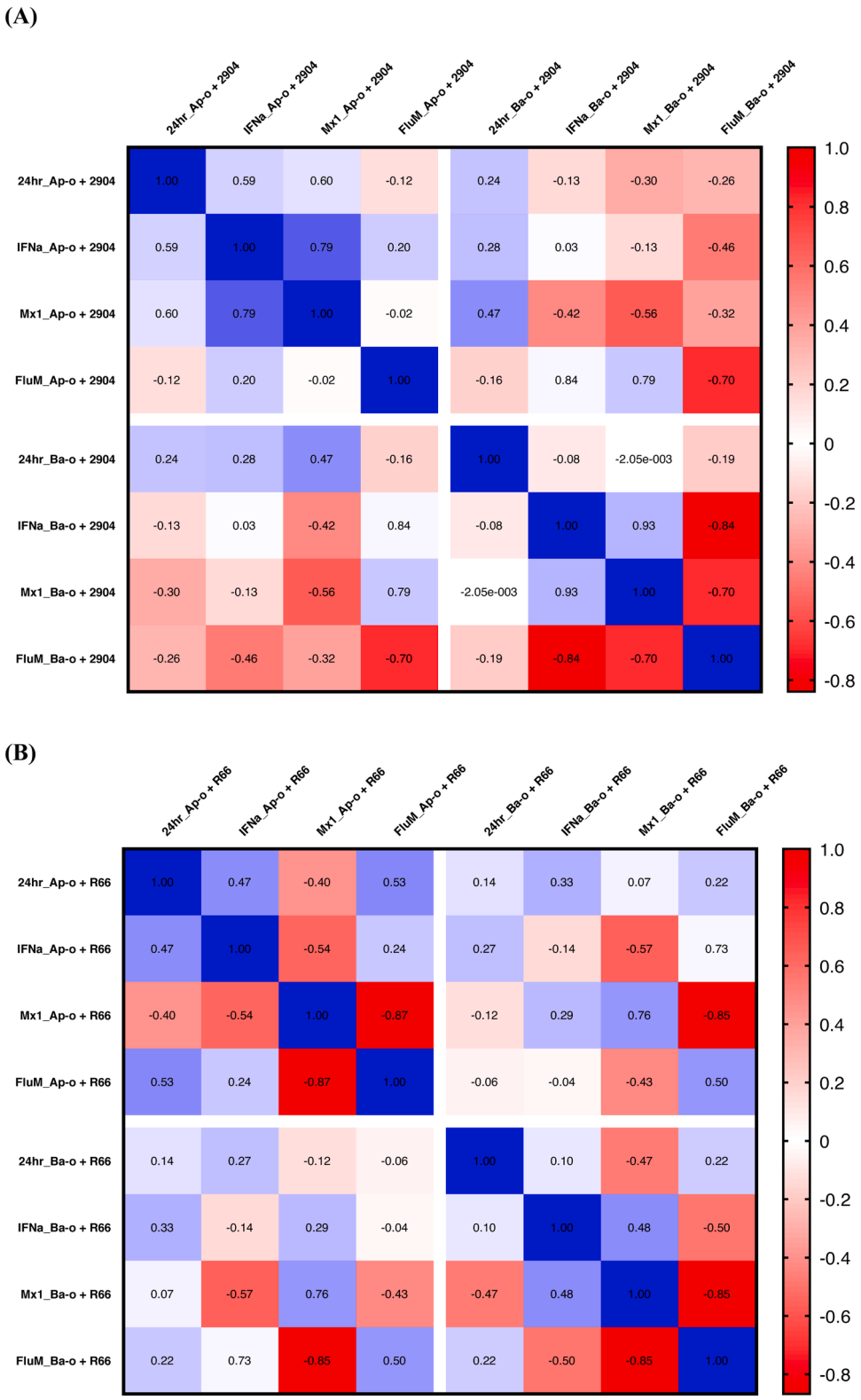

Fig. 7. Correlation matrix of viral titers and qRT-PCR results in LPAIV-infected CIOs. Pearson's correlation analysis was performed using GraphPad Prism 9 to assess the relationship between viral titers and innate immune responses. The correlation matrices represent data from H6N1-2904 (A) and H9N2-R66 (B) at 24 h post-infection. All analyses were conducted using parametric Pearson's two-tailed correlation with a 95 % confidence interval.

(Kimble, et al., 2010).

For instance, H6N1 from the Taiwan clade I can reach titers of 10^4 TCID50/mL in the lungs of infected mice while showing minimal effects in chickens. In contrast, the H6N1-2904 Taiwan isolate used in this study, classified as clade II similar to its ancestor, the Goose/Guangdong (GS/GD) lineage (Croville, et al., 2012), which is hard to interpret in mouse models, as it fails to replicate in the lungs of BALB/c mice. Thus, the differences in pathogenicity between H6 subtypes cannot be easily

explained using the mouse infection model alone (Huang, et al., 2017; Lee, et al., 2006).

In vitro models, particularly chicken intestinal organoids (CIOs), have confirmed the GI tract as a consistent site of LPAIV replication (Kaiser, et al., 2017). CIOs accurately represent avian intestinal epithelium, where H6N1 achieves robust replication, highlighting its adaptation to the gut environment (Beaumont, et al., 2021). The high viral replication observed in these models aligns with *in vivo* findings, reinforcing the hypothesis that the GI tract serves as the primary niche for LPAIV replication. Available data indicate that H6N1 primarily replicates in the intestinal system, where viral RNA and antigens are consistently detected in the gastrointestinal tract of poultry, with limited evidence of replication in other organs (Lee, et al., 2006). However, studies have shown that H6N1 variants carrying the HA G228S mutation exhibit enhanced nephrotropism, leading to viral replication in the kidneys and associated interstitial nephritis (Tu, et al., 2022; Wang and Wang, 2003). This shift in understanding underscores the importance of GI tropism in LPAIV biology and provides more precise insights into the mechanisms that allow the virus to persist in avian hosts.

The development of chicken intestinal organoids (CIOs) represents a significant advancement in avian virology. While mammalian intestinal organoid cultures typically utilize Gastrin to promote growth, studies have shown that this growth factor has limited efficacy in avian systems. Instead, Prostaglandin E2 (PGE2) plays a crucial role in supporting the growth and proliferation of avian organoids, including CIOs (Pierzchalska, et al., 2012). Unlike Gastrin, which primarily regulates the BMP signaling pathway to maintain mammalian organoid growth, PGE2 exerts its effects through the Wnt signaling pathway, promoting β-catenin stabilization by inhibiting GSK3β (Powell and Behnke, 2017). This leads to enhanced intestinal stem cell (ISC) expansion and epithelial regeneration, particularly in response to tissue damage (Holmberg, et al., 2017). Additionally, PGE2 enhances cell proliferation by activating PGE2-R subunits, which trigger cAMP/PKA and PI3K/AKT signaling pathways, crucial for maintaining intestinal epithelial homeostasis (Stelzner, et al., 2012). Our results demonstrate that PGE2 more effectively supports the proliferation of avian intestinal epithelial cells compared to Gastrin, highlighting the species-specific growth requirements of avian tissues (Altay, et al., 2019). Furthermore, our study emphasizes that while Gastrin and PGE2 facilitate intestinal regeneration, their mechanisms of action differ significantly, with PGE2′s activation of the Wnt pathway proving more critical for avian intestinal organoid development (Oost, et al., 2022; Zhao, et al., 2022).

The formation of Ap-o and Ba-o organoids represents the directional orientation of epithelial cells and their interaction with pathogens (Nash, et al., 2021). In our results, when using Caco-2 organoids, a human intestinal epithelial model, LPAIV replication was significantly higher in Ap-o organoids compared to Ba-o organoids. This may be attributed to the presence of membrane-bound proteases on the apical surface that facilitate viral entry, such as TMPRSS2, which had shown a strong correlation to H6 infection in mice (Bestle, et al., 2021) and is highly expressed in Caco-2 cells (Saccon, et al., 2021; Shuai, et al., 2020). However, the opposite trend was observed in chicken intestinal organoids, suggesting that species-specific differences in intestinal epithelial composition and protease availability influence viral replication dynamics. In comparison, CIOs demonstrated differential susceptibilities to infection, reinforcing the role of proteases in modulating viral replication efficiency may vary depending on the organoid's orientation and cell origin, especially when the membrane-bound proteases play a curial role. Nevertheless, the contrasting results between human and chicken intestinal organoids suggest that species-specific epithelial characteristics, rather than orientation alone, should be considered as the main player in viral replication efficiency when discussing LPAIVs.

The innate immune response plays a pivotal role in the outcome of IAV infections, acting as the first line of defense against viral invasion (Shin, et al., 2020). Upon infection, host cells recognize viral components through pattern recognition receptors (PRRs) such as RIG-I and MDA5, triggering downstream signaling pathways that produce type I interferons (IFNs). These IFNs, in turn, induce the expression of interferon-stimulated genes (ISGs) like *Mx1*, which inhibit viral replication (Deblanc, et al., 2016). Our study observed that the H6N1-2904 strain was associated with a robust ISG response in Ap-o organoids, which correlated with lower viral titers in these organoids (Fig. 6). In contrast, the H9N2-R66 strain exhibited higher viral titers in Ba-o organoids, where the ISG response was less pronounced. While no direct statistical comparison between H6N1 and H9N2 infections was performed within the same organoid orientation, trends from Fig. 4 suggest that H6N1 replication in Ap-o organoids was lower than in Ba-o organoids. To further support this observation, Pearson's r-correlation analysis (Fig. 7) demonstrated a statistically significant inverse correlation between ISG expression and viral titers in multiple conditions, including H9N2-R66 infected Ap-o organoids, Ba-o organoids and H6N1-2904 infected Ba-o organoids. These findings suggest that strain-specific innate immune activation, rather than organoid orientation alone, influences viral replication dynamics in intestinal organoid models. This suggests that Ap-o organoids, which simulate infection from the intestinal lumen, are more effective at mounting an antiviral response compared to Ba-o organoids, which mimic systemic infection via the bloodstream. The observed difference in ISG response between the two orientations suggests that IAVs may employ distinct immune evasion strategies depending on the entry route.

These findings align with previous observations in swine models, where certain IAV strains replicate efficiently despite a limited or restricted interferon-driven innate immune response, possibly due to modulation of the JAK/STAT signaling pathway (Bakre, et al., 2021; Delgado-Ortega, et al., 2014). The ability of IAVs to manipulate host immune responses, particularly by evading or suppressing the innate immune response, is a critical factor in their pathogenicity and persistence in the host (Weber, et al., 2004). In our study, we focus on *in vitro* organoid models providing a controlled system for virus-host interactions. Compared to *ex vivo* chicken intestinal tissues, LPAIV replication has shown variable trends in chicken precision-cut intestinal slices, showing that the influence from residential elements, such as immunocyte or gut microbiota, cannot easily be waived (Punyadarsaniya, et al., 2015). For instance, an *in vivo* study had shown that microbial depletion in chicken gut may downregulate IFN-I-related ISG expression, impacting antiviral defenses (Yitbarek, et al., 2018). Given these factors, future studies targeting how resident microbiota affect LPAIV infection dynamics and ISG regulation in the established organoids model would be essential. Additionally, further applications toward antiviral agents and health integrates, or plant extracts against LPAIV could be fulfilled without extensive laboratory animal use. Applying Ap-o and Ba-o CIOs and focusing on innate immunity dynamics accurately represents virus-host interactions, contributing to improved biosecurity in local poultry industries and informing strategies to control avian influenza.

We thank Ching-Ho Wang (National Taiwan University, Taipei City, Taiwan), and Georg Herrler (University of Veterinary Medicine Hannover, Hannover, Germany) for kindly providing viral strains.

Disclosures

The authors declare no conflict of interest in the present study.

CRediT authorship contribution statement

Dai-Lun Shin: Conceptualization, Formal analysis, Investigation, Methodology, Resources, Writing – original draft, Writing – review & editing, Funding acquisition. **Yi-Bei Tsai:** Investigation, Methodology, Writing – review & editing. **Shu-Han Hsu:** Investigation, Writing – review & editing. **Chi-Chia Liang:** Investigation, Writing – review & editing. **Nai-Huei Wu:** Conceptualization, Formal analysis,

Investigation, Methodology, Resources, Writing – original draft, Writing – review & editing, Funding acquisition.

Declaration of competing interest

The authors declare that they have no known competing financial interests or personal relationships that could have appeared to influence the work reported in this paper.

Acknowledgments

Funding: This work was supported by the National Science and Technology Council (NSTC, former MOST) [MOST 110-2313-B-002-003-MY3, NSTC 112-2313-B-002-041-MY3, NSTC 113-2313-B-005-004-MY3]; the National Taiwan University within the framework of the Higher Education Sprout Project by the Ministry of Education (MOE) in Taiwan [NTU-113L7804, NTU-114L7864].

References

Abd El-Hack, M.E., El-Saadony, M..T., Alqhtani, A.H., Swelum, A.A., Salem, H.M., Elbestawy, A.R., Noreldin, A.E., Babalghith, A.O., Khafaga, A.F., Hassan, M.I., El-Tarabily, K.A., 2022. The relationship among avian influenza, gut microbiota and chicken immunity: an updated overview. Poult. Sci. 101, 102021. https://doi.org/10.1016/j.psj.2022.102021.

Altay, G., Larranaga, E., Tosi, S., Barriga, F.M., Batlle, E., Fernandez-Majada, V., Martinez, E., 2019. Self-organized intestinal epithelial monolayers in crypt and villus-like domains show effective barrier function. Sci. Rep. 9, 10140. https://doi.org/10.1038/s41598-019-46497-x.

Bakre, A.A., Jones, L..P., Murray, J., Reneer, Z.B., Meliopoulos, V.A., Cherry, S., Schultz-Cherry, S., Tripp, R.A., 2021. Innate antiviral cytokine response to swine influenza virus by swine respiratory epithelial cells. J. Virol. 95, e0069221. https://doi.org/10.1128/jvi.00692-21.

Baron, J., Tarnow, C., Mayoli-Nussle, D., Schilling, E., Meyer, D., Hammami, M., Schwalm, F., Steinmetzer, T., Guan, Y., Garten, W., Klenk, H.D., Bottcher-Friebertshauser, E., 2013. Matriptase, HAT, and TMPRSS2 activate the hemagglutinin of H9N2 influenza A viruses. J. Virol. 87, 1811–1820. https://doi.org/10.1128/JVI.02320-12.

Bazzigher, L., Schwarz, A., Staeheli, P., 1993. No enhanced influenza virus resistance of murine and avian cells expressing cloned duck Mx protein. Virology. 195, 100–112. https://doi.org/10.1006/viro.1993.1350.

Beaumont, M., Blanc, F., Cherbuy, C., Egidy, G., Giuffra, E., Lacroix-Lamande, S., Wiedemann, A., 2021. Intestinal organoids in farm animals. Vet. Res. 52, 33. https://doi.org/10.1186/s13567-021-00909-x.

Bestle, D., Limburg, H., Kruhl, D., Harbig, A., Stein, D.A., Moulton, H., Matrosovich, M., Abdelwhab, E.M., Stech, J., Böttcher-Friebertshäuser, E., 2021. Hemagglutinins of avian influenza viruses are proteolytically activated by TMPRSS2 in Human and murine airway cells. J. Virol. 95, e0090621. https://doi.org/10.1128/jvi.00906-21.

Brauer, R., Chen, P., 2015. Influenza virus propagation in embryonated chicken eggs. J. Vis. Exp. e52421. https://doi.org/10.3791/52421.

Chen, B., Slocombe, R.F., Georgy, S.R., 2023. Advances in organoid technology for veterinary disease modeling. Front. Vet. Sci. 10, 1234628. https://doi.org/10.3389/fvets.2023.1234628.

Croville, G., Soubies, S.M., Barbieri, J., Klopp, C., Mariette, J., Bouchez, O., Camus-Bouclainville, C., Guerin, J.L., 2012. Field monitoring of avian influenza viruses: whole-genome sequencing and tracking of neuraminidase evolution using 454 pyrosequencing. J. Clin. Microbiol. 50, 2881–2887. https://doi.org/10.1128/JCM.01142-12.

Deblanc, C., Delgado-Ortega, M., Gorin, S., Berri, M., Paboeuf, F., Berthon, P., Herrler, G., Meurens, F., Simon, G., 2016. Mycoplasma hyopneumoniae does not affect the interferon-related anti-viral response but predisposes the pig to a higher level of inflammation following swine influenza virus infection. J. Gen. Virol. 97, 2501–2515. https://doi.org/10.1099/jgv.0.000573.

Delgado-Ortega, M., Melo, S., Punyadarsaniya, D., Rame, C., Olivier, M., Soubieux, D., Marc, D., Simon, G., Herrler, G., Berri, M., Dupont, J., Meurens, F., 2014. Innate immune response to a H3N2 subtype swine influenza virus in newborn porcine trachea cells, alveolar macrophages, and precision-cut lung slices. Vet. Res. 45, 42. https://doi.org/10.1186/1297-9716-45-42.

Fouchier, R.A., Bestebroer, T..M., Herfst, S., Van Der Kemp, L., Rimmelzwaan, G.F., Osterhaus, A.D., 2000. Detection of influenza A viruses from different species by PCR amplification of conserved sequences in the matrix gene. J. Clin. Microbiol. 38, 4096–4101. https://doi.org/10.1128/JCM.38.11.4096-4101.2000.

Ge, S., Wang, Z., 2011. An overview of influenza a virus receptors. Crit. Rev. Microbiol. 37, 157–165. https://doi.org/10.3109/1040841X.2010.536523.

Gohrbandt, S., Veits, J., Breithaupt, A., Hundt, J., Teifke, J.P., Stech, O., Mettenleiter, T. C., Stech, J., 2011. H9 avian influenza reassortant with engineered polybasic cleavage site displays a highly pathogenic phenotype in chicken. J. Gen. Virol. 92, 1843–1853. https://doi.org/10.1099/vir.0.031591-0.

Hassanpour, H., Bahadoran, S., Farhadfar, F., Chamali, Z.F., Nazari, H., Kaewduangta, W., 2018. Identification of reliable reference genes for quantitative real-time PCR in lung and heart of pulmonary hypertensive chickens. Poult. Sci. 97, 4048–4056. https://doi.org/10.3382/ps/pey258.

Holmberg, F.E., Seidelin, J..B., Yin, X., Mead, B.E., Tong, Z., Li, Y., Karp, J.M., Nielsen, O. H., 2017. Culturing human intestinal stem cells for regenerative applications in the treatment of inflammatory bowel disease. EMBo Mol. Med. 9, 558–570. https://doi.org/10.15252/emmm.201607260.

Huang, L., Hou, Q., Ye, L., Yang, Q., Yu, Q., 2017. Crosstalk between H9N2 avian influenza virus and crypt-derived intestinal organoids. Vet. Res. 48, 71. https://doi.org/10.1186/s13567-017-0478-6.

Ito, T., Suzuki, Y., Takada, A., Kawamoto, A., Otsuki, K., Masuda, H., Yamada, M., Suzuki, T., Kida, H., Kawaoka, Y., 1997. Differences in sialic acid-galactose linkages in the chicken egg amnion and allantois influence human influenza virus receptor specificity and variant selection. J. Virol. 71, 3357–3362. https://doi.org/10.1128/jvi.71.4.3357-3362.1997.

Kaiser, A., Willer, T., Steinberg, P., Rautenschlein, S., 2017. Establishment of an *In vitro* intestinal epithelial cell culture model of Avian origin. Avian Dis. 61, 229–236. https://doi.org/10.1637/11524-110216-Reg.1.

Kalthoff, D., Globig, A., Beer, M., 2010. (Highly pathogenic) avian influenza as a zoonotic agent. Vet. Microbiol. 140, 237–245. https://doi.org/10.1016/j.vetmic.2009.08.022.

Kanrai, P., Mostafa, A., Madhugiri, R., Lechner, M., Wilk, E., Schughart, K., Ylosmaki, L., Saksela, K., Ziebuhr, J., Pleschka, S., 2016. Identification of specific residues in avian influenza A virus NS1 that enhance viral replication and pathogenicity in mammalian systems. J. Gen. Virol. 97, 2135–2148. https://doi.org/10.1099/jgv.0.000542.

Kimble, B., Nieto, G.R., Perez, D.R., 2010. Characterization of influenza virus sialic acid receptors in minor poultry species. Virol. J. 7, 365. https://doi.org/10.1186/1743-422x-7-365.

Ko, J.H., Jin, H..K., Asano, A., Takada, A., Ninomiya, A., Kida, H., Hokiyama, H., Ohara, M., Tsuzuki, M., Nishibori, M., Mizutani, M., Watanabe, T., 2002. Polymorphisms and the differential antiviral activity of the chicken Mx gene. Genome Res. 12, 595–601. https://doi.org/10.1101/gr.210702.

Lee, D.H., Bertran, K.., Kwon, J.H., Swayne, D.E., 2017. Evolution, global spread, and pathogenicity of highly pathogenic avian influenza H5Nx clade 2.3.4.4. J. Vet. Sci. 18, 269–280. https://doi.org/10.4142/jvs.2017.18.S1.269.

Lee, M.S., Chang, P..C., Shien, J.H., Cheng, M.C., Chen, C.L., Shieh, H.K., 2006. Genetic and pathogenic characterization of H6N1 avian influenza viruses isolated in Taiwan between 1972 and 2005. Avian Dis. 50, 561–571. https://doi.org/10.1637/7640-050106r.1.

Lee, Y.S., Lee, S..H., Gadde, U.D., Oh, S.T., Lee, S.J., Lillehoj, H.S., 2018. Allium hookeri supplementation improves intestinal immune response against necrotic enteritis in young broiler chickens. Poult. Sci. 97, 1899–1908. https://doi.org/10.3382/ps/pey031.

Li, Z., Wang, Y., Li, X., Li, X., Cao, H., Zheng, S.J., 2013. Critical roles of glucocorticoid-induced leucine zipper in infectious bursal disease virus (IBDV)-induced suppression of type I interferon expression and enhancement of IBDV growth in host cells via interaction with VP4. J. Virol. 87, 1221–1231. https://doi.org/10.1128/JVI.02421-12.

Mostafa, A., Abdelwhab, E.M., Mettenleiter, T.C., Pleschka, S., 2018. Zoonotic potential of influenza A viruses: a comprehensive overview. Viruses. 10, 497. https://doi.org/10.3390/v10090497.

Nash, T., Vervelde, L., 2022. Advances, challenges and future applications of avian intestinal *in vitro* models. Avian Pathol. 51, 317–329. https://doi.org/10.1080/03079457.2022.2084363.

Nash, T.J., Morris, K..M., Mabbott, N.A., Vervelde, L., 2021. Inside-out chicken enteroids with leukocyte component as a model to study host-pathogen interactions. Commun. Biol. 4, 377. https://doi.org/10.1038/s42003-021-01901-z.

Oost, M.J., Ijaz, A.., van Haarlem, D.A., van Summeren, K., Velkers, F.C., Kraneveld, A. D., Venema, K., Jansen, C.A., Pieters, R.H.H., Ten Klooster, J.P., 2022. Chicken-derived RSPO1 and WNT3 contribute to maintaining longevity of chicken intestinal organoid cultures. Sci. Rep. 12, 10563. https://doi.org/10.1038/s41598-022-14875-7.

Ou, S.C., 2003. Study on the Pathogenic and Molecular Evolution of Avian Influenza Viruses Subtype H6N1 in Experimental and Field Chickens. Master of Veterinary Medicine. National Chung Hsing University, Taichung, Taiwan.

Peacock, T.P., Sealy, J..E., Harvey, W.T., Benton, D.J., Reeve, R., Iqbal, M., 2021. Genetic determinants of receptor-binding preference and zoonotic potential of H9N2 avian influenza viruses. J. Virol. 95, e01651–20. https://doi.org/10.1128/jvi.01651-20.

Penski, N., Härtle, S., Rubbenstroth, D., Krohmann, C., Ruggli, N., Schusser, B., Pfann, M., Reuter, A., Gohrbandt, S., Hundt, J., Veits, J., Breithaupt, A., Kochs, G., Stech, J., Summerfield, A., Vahlenkamp, T., Kaspers, B., Staeheli, P., 2011. Highly pathogenic avian influenza viruses do not inhibit interferon synthesis in infected chickens but can override the interferon-induced antiviral state. J. Virol. 85, 7730–7741. https://doi.org/10.1128/jvi.00063-11.

Pierzchalska, M., Grabacka, M., Michalik, M., Zyla, K., Pierzchalski, P., 2012. Prostaglandin E2 supports growth of chicken embryo intestinal organoids in Matrigel matrix. Biotechniques 52, 307–315. https://doi.org/10.2144/0000113851.

Powell, R.H., Behnke, M.S., 2017. WRN conditioned media is sufficient for propagation of intestinal organoids from large farm and small companion animals. Biol. Open. 6, 698–705. https://doi.org/10.1242/bio.021717.

Punyadarsaniya, D., Winter, C., Mork, A.K., Amiri, M., Naim, H.Y., Rautenschlein, S., Herrler, G., 2015. Precision-cut intestinal slices as a culture system to analyze the infection of differentiated intestinal epithelial cells by avian influenza viruses. J. Virol. Methods 212, 71–75. https://doi.org/10.1016/j.jviromet.2014.10.015.

Saccon, E., X. Chen, F. Mikaeloff, J. E. Rodriguez, L. Szekely, B. S. Vinhas, S. Krishnan, S. N. Byrareddy, T. Frisan, Á. Végvári, A. Mirazimi, U. Neogi, and S. Gupta. 2021. Cell-

type-resolved quantitative proteomics map of interferon response against SARS-CoV-2. iScience 24:102420. doi 10.1016/j.isci.2021.102420.
Santhakumar, D., Rubbenstroth, D., Martinez-Sobrido, L., Munir, M., 2017. Avian interferons and their antiviral effectors. Front. Immunol. 8, 49. https://doi.org/10.3389/fimmu.2017.00049.
Shin, D.L., Yang, W.., Peng, J.Y., Sawatsky, B., von Messling, V., Herrler, G., Wu, N.H., 2020. Avian Influenza A virus infects swine airway epithelial cells without prior adaptation. Viruses. 12, 589. https://doi.org/10.3390/v12060589.
Shinya, K., Ebina, M., Yamada, S., Ono, M., Kasai, N., Kawaoka, Y., 2006. Avian flu: influenza virus receptors in the human airway. Nature 440, 435–436. https://doi.org/10.1038/440435a.
Shuai, H., Chu, H., Hou, Y., Yang, D., Wang, Y., Hu, B., Huang, X., Zhang, X., Chai, Y., Cai, J.P., Chan, J.F., Yuen, K.Y., 2020. Differential immune activation profile of SARS-CoV-2 and SARS-CoV infection in human lung and intestinal cells: implications for treatment with IFN-β and IFN inducer. J. Infect. 81, e1–e10. https://doi.org/10.1016/j.jinf.2020.07.016.
Spackman, E., 2023. A review of the stability of Avian Influenza Virus in materials from poultry farms. Avian Dis. 67, 229–236. https://doi.org/10.1637/aviandiseases-D-23-00027.
Stelzner, M., Helmrath, M., Dunn, J.C., Henning, S.J., Houchen, C.W., Kuo, C., Lynch, J., Li, L., Magness, S.T., Martin, M.G., Wong, M.H., Yu, J., Consortium, N.I.H.I.S.C., 2012. A nomenclature for intestinal *in vitro* cultures. Am. J. Physiol.. Gastrointestin. Liver Physiol. 302, G1359–G1363. https://doi.org/10.1152/ajpgi.00493.2011.
Takeuchi, O., Akira, S., 2010. Pattern recognition receptors and inflammation. Cell 140, 805–820. https://doi.org/10.1016/j.cell.2010.01.022.
Tu, F.E., Hu, S..C., Cheng, I.C., Hsu, W.C., Chen, Y.W., Chen, L.H., 2022. Pathogenesis of low pathogenic avian influenza virus subtype H6N1 infection in chickens. Exp. Rep. AHRI 56, 10.
Umar, S., Guerin, J.L., Ducatez, M.F., 2017. Low pathogenic Avian influenza and coinfecting pathogens: a review of experimental infections in Avian models. Avian Dis. 61, 3–15. https://doi.org/10.1637/11514-101316-Review.
Verhagen, J.H., Fouchier, R.A.M., Lewis, N., 2021. Highly pathogenic avian influenza viruses at the wild-domestic bird interface in Europe: future directions for research and surveillance. Viruses. 13. https://doi.org/10.3390/v13020212.
Wang, C.W., Wang, C.H., 2003. Experimental selection of virus derivatives with variations in virulence from a single low-pathogenicity H6N1 avian influenza virus field isolate. Avian Dis. 47, 1416–1422. https://doi.org/10.1637/6093.
Weber, F., Kochs, G., Haller, O., 2004. Inverse interference: how viruses fight the interferon system. Viral. Immunol. 17, 498–515. https://doi.org/10.1089/vim.2004.17.498.
Weerts, E., Bouwman, K.M., Paerels, L., Grone, A., Boelm, G.J., Verheije, M.H., 2022. Interference between avian corona and influenza viruses: the role of the epithelial architecture of the chicken trachea. Vet. Microbiol. 272, 109499. https://doi.org/10.1016/j.vetmic.2022.109499.
Wei, S.H., Yang, J..R., Wu, H.S., Chang, M.C., Lin, J.S., Lin, C.Y., Liu, Y.L., Lo, Y.C., Yang, C.H., Chuang, J.H., Lin, M.C., Chung, W.C., Liao, C.H., Lee, M.S., Huang, W.T., Chen, P.J., Liu, M.T., Chang, F.Y., 2013. Human infection with avian influenza A H6N1 virus: an epidemiological analysis. Lancet Respir. Med. 1, 771–778. https://doi.org/10.1016/S2213-2600(13)70221-2.
Wilk, E., Schughart, K., 2012. The mouse as model system to study host-pathogen interactions in Influenza A infections. Curr. Protoc. Mouse Biol. 2, 177–205. https://doi.org/10.1002/9780470942390.mo110173.
Wu, N.H., Meng, F.., Seitz, M., Valentin-Weigand, P., Herrler, G., 2015. Sialic acid-dependent interactions between influenza viruses and Streptococcus suis affect the infection of porcine tracheal cells. J. Gen. Virol. 96, 2557–2568. https://doi.org/10.1099/jgv.0.000223.
Wu, N.H., Yang, W.., Beineke, A., Dijkman, R., Matrosovich, M., Baumgartner, W., Thiel, V., Valentin-Weigand, P., Meng, F., Herrler, G., 2016. The differentiated airway epithelium infected by influenza viruses maintains the barrier function despite a dramatic loss of ciliated cells. Sci. Rep. 6, 39668. https://doi.org/10.1038/srep39668.
Yamaji, R., Saad, M.D., Davis, C.T., Swayne, D.E., Wang, D., Wong, F.Y.K., McCauley, J. W., Peiris, J.S.M., Webby, R.J., Fouchier, R.A.M., Kawaoka, Y., Zhang, W., 2020. Pandemic potential of highly pathogenic avian influenza clade 2.3.4.4 A(H5) viruses. Rev. Med. Virol. 30, e2099. https://doi.org/10.1002/rmv.2099.
Yang, W., Punyadarsaniya, D., Lambertz, R.L.O., Lee, D.C.C., Liang, C.H., Hoper, D., Leist, S.R., Hernandez-Caceres, A., Stech, J., Beer, M., Wu, C.Y., Wong, C.H., Schughart, K., Meng, F., Herrler, G., 2017. Mutations during the adaptation of H9N2 Avian Influenza Virus to the Respiratory epithelium of pigs enhance sialic acid binding activity and virulence in mice. J. Virol. 91, e02125–16. https://doi.org/10.1128/JVI.02125-16.
Yitbarek, A., Alkie, T., Taha-Abdelaziz, K., Astill, J., Rodriguez-Lecompte, J.C., Parkinson, J., Nagy, É., Sharif, S., 2018. Gut microbiota modulates type I interferon and antibody-mediated immune responses in chickens infected with influenza virus subtype H9N2. Benef. Microbes. 9, 417–427. https://doi.org/10.3920/bm2017.0088.
Zhao, D., Farnell, M.B., Kogut, M.H., Genovese, K.J., Chapkin, R.S., Davidson, L.A., Berghman, L.R., Farnell, Y.Z., 2022. From crypts to enteroids: establishment and characterization of avian intestinal organoids. Poult. Sci. 101, 101642. https://doi.org/10.1016/j.psj.2021.101642.